

Published in final edited form as:

Cell. 2012 October 26; 151(3): 658–670. doi:10.1016/j.cell.2012.08.043.

Unraveling inflammatory responses using systems genetics and gene-environment interactions in macrophages

Luz D. Orozco^{*1}, Brian J. Bennett^{*2}, Charles R. Farber³, Anatole Ghazalpour², Calvin Pan¹, Nam Che², Pingzi Wen², Hong Xiu Qi², Adonisa Mutukulu⁴, Nathan Siemers⁵, Isaac Neuhaus⁵, Roumyana Yordanova⁶, Peter Gargalovic⁷, Matteo Pellegrini⁸, Todd Kirchgessner⁷, and Aldons J. Lusis^{1,2}

¹Department of Human Genetics; University of California, Los Angeles; Los Angeles, California, 90095; USA

²Department of Medicine; David Geffen School of Medicine, University of California, Los Angeles; Los Angeles, California, 90095; USA

³Department of Medicine; University of Virginia; Charlottesville, Virginia, 22908; USA

⁴Department of Biochemistry; University of California, Los Angeles; Los Angeles, California, 90095; USA

⁵Department of Bioinformatics & Proteomics; Bristol-Myers Squibb; Pennington, New Jersey, 08534; USA

⁶Department of Applied Genomics; Bristol-Myers Squibb; Pennington, New Jersey, 08534; USA

⁷Department of Atherosclerosis Drug Discovery; Bristol-Myers Squibb; Pennington, New Jersey, 08534; USA

⁸Department of Molecular, Cell and Developmental Biology; University of California, Los Angeles; Los Angeles, California, 90095; USA

SUMMARY

Many common diseases have an important inflammatory component mediated in part by macrophages. Here we used a systems genetics strategy to examine the role of common genetic variation in macrophage responses to inflammatory stimuli.

We examined genome-wide transcript levels in macrophages from 92 strains of the Hybrid Mouse Diversity Panel. We exposed macrophages to control media, bacterial lipopolysaccharide, or oxidized phospholipids. We performed association mapping under each condition and identified several thousand expression quantitative trait loci (eQTL), gene-by-environment interactions and several eQTL “hotspots” that specifically control LPS responses. We validated an eQTL hotspot in chromosome 8 using siRNA knock-down of candidate genes and identified the gene *2310061C15Rik*, as a novel regulator of inflammatory responses in macrophages.

© 2012 Elsevier Inc. All rights reserved.

Contact: Luz D. Orozco, 3000 Terasaki Life Sciences Building, 610 Charles Young Drive East, Los Angeles, CA 90095, USA, luz.d.orozco@gmail.com, ldorozco@mednet.ucla.edu.

* Authors contributed equally

Publisher's Disclaimer: This is a PDF file of an unedited manuscript that has been accepted for publication. As a service to our customers we are providing this early version of the manuscript. The manuscript will undergo copyediting, typesetting, and review of the resulting proof before it is published in its final citable form. Please note that during the production process errors may be discovered which could affect the content, and all legal disclaimers that apply to the journal pertain.

We have created a public database where the data presented here can be used as a resource for understanding many common inflammatory traits which are modeled in the mouse, and for the dissection of regulatory relationships between genes.

INTRODUCTION

After the completion of the Human Genome Project and the HapMap project, the field of genetics witnessed an explosion of genome-wide association studies that aimed to identify the common variants that affect common diseases in humans. Despite this effort, accumulating data have shown that all identified loci combined can only explain a small fraction of the variation in the population. This has been speculated to be partly due to environmental factors and their interaction with various genes influencing the traits. Therefore, uncovering such gene-by-environment interactions (GxE) will aid in understanding the mechanisms underlying the observed variation in the population. In an effort to elucidate such interactions, we focused on inflammation and sought to determine to what extent environmental factors that trigger immunological responses interact with naturally occurring variation to determine the phenotypic outcomes.

Inflammation is the innate immune response to harmful stimuli such as pathogens, injury and tissue malfunction. *Acute inflammation* is associated with the response to infection and tissue injury, and is often triggered by recognition of bacterial products such as lipopolysaccharide (LPS). In contrast, *chronic inflammation* is thought to be the underlying cause of many complex diseases, including autoimmune disease (Kanter et al., 2006), Alzheimer's disease (Rojo et al., 2006) and atherosclerosis (Berliner et al., 2009). We and others have shown that oxidized phospholipids, such as oxidized 1-palmitoyl-2-arachidonoyl-sn-glycero-3-phosphatidylcholine (OxPAPC), are potent environmental stimuli which can trigger the initial recruitment of macrophages, and contribute to both initiation and progression of chronic inflammation (Berliner et al., 2009).

Genetic variation in naturally occurring populations can have dramatic effects on how individuals respond to environmental stimuli such as LPS and OxPAPC. Studies in model organisms have revealed thousands of GxE interactions responsible for phenotypic differences among genetically diverse individuals (Smith and Kruglyak, 2008). Wurfel *et al.* demonstrated in humans that some individuals show high sensitivity to LPS, while others exhibit low sensitivity (Wurfel et al., 2005), suggesting that GxE interactions play a role in the extent of inflammatory responses. Similarly, chronic inflammatory conditions such as atherosclerosis are influenced by both genetic and environmental variation, and multiple studies suggest that GxE interactions are an important component of the disease etiology (Romanoski et al., 2010).

In this study, we sought to understand macrophage inflammatory responses and how these are influenced by genetics in a panel of genetically diverse mouse inbred strains called the Hybrid Mouse Diversity Panel (HMDP). We obtained primary macrophages from each of the strains and exposed them to inflammatory stimuli. We then profiled the transcriptome and used genome-wide association to reveal genetic loci and GxE interactions in the macrophage response to inflammatory stimuli. All our results are publicly available through our database website <http://systems.genetics.ucla.edu/data>. Here we will describe our results and demonstrate how the analyses and data we generated can be exploited to further our understanding of cellular processes involved in macrophage inflammation.

RESULTS

Macrophage HMDP samples

To better understand inflammatory responses in macrophages, we obtained primary macrophages from 92 mouse inbred strains of the HMDP. We exposed the cells to control media, LPS, or OxPAPC and measured genome-wide mRNA expression levels using microarrays. To determine reproducibility, we also examined expression levels from seven strains in the control condition, and five strains in the LPS condition at different times, using different mice of the same strain to examine biological reproducibility. We used hierarchical clustering of data for all genes in the microarray and found that samples of the same strain clustered together independent of the experiment date, suggesting that genome-wide expression levels were highly reproducible for both experimental and biological replicates (Figure S1, A and B). As an example, the variation in the response to LPS of *Ccl2* (MCP-1) is shown in Figure S1C.

If the variation in gene expression between samples of the same strain was comparable to variation among different strains, this would lead to false positive results due to random fluctuations in gene expression levels. To examine this possibility, we compared the distribution of the variance in gene expression among different strains (inter-strain variance), to the variance in samples from the same strain (intra-strain variance). We found that the inter-strain variance was 2.2-fold larger than the intra-strain variance in strain BXH20/KccJ ($p=1.26\times 10^{-226}$, Figure S1D), with similar results in additional strains, where the inter-strain variance was larger than the intra-strain variance by 2-fold in BXA12/PgnJ ($p=0$), 2.5-fold larger in BXD33/TyJ ($p=9.99\times 10^{-270}$), 2.4-fold larger in BXD36/TyJ ($p=8.49\times 10^{-309}$), and 2.3-fold larger in LG/J ($p=0$).

We carried out expression array profiling in macrophages from 92 strains out of the 100 strains originally included in the HMDP. To ensure that we did not introduce a bias due to possible differences in cell viability in response to an inflammatory stimulus, we examined viability using calcein AM, which produces an intense fluorescence in live but not in dead cells (Figure S2). We found no significant differences in viability after LPS treatment ($p=0.76$) between cells from strains included (93.6%) and strains not included in this study (94.9%).

Genetic, environmental and GxE interactions

We examined the effect of genetic differences, environmental stimuli and GxE interactions on global gene expression levels using analysis of variance (Anova). We found that 5,726 (44.1%) out of 12,980 genes represented in the array were under genetic regulation at the 5% FDR rate (Table S1). For environmental effects, we compared control versus treated (LPS or OxPAPC) samples, and found that 2,802 (21.6%) genes were regulated by LPS, 593 (4.6%) genes were regulated by OxPAPC, and 2,946 genes (22.7%) were regulated by at least one of the treatments over 2-fold. There was a significant overlap of 445 genes that were differentially expressed over 2-fold in both treatments ($p<1.0\times 10^{-16}$).

In a genetically diverse population such as our panel of strains, GxE interactions can be observed when a strain(s) responds to a given environmental stimulus (e.g. LPS), while another strain(s) of different genetic background does not. We found GxE interactions in 2,607 (20.1%) genes in LPS-treated cells, 512 (3.9%) genes in OxPAPC treated cells, and 2,786 (21.5%) genes that showed a GxE interaction in at least one of the conditions. Although treatment influenced expression levels in a larger number of genes for LPS than for OxPAPC treatment, a large proportion of the genes differentially expressed show GxE

interactions in both LPS (2607/2802, 93%) and OxPAPC (512/593, 86%) treatments. The total number of genes regulated, and genes regulated over 2-fold is shown in Table S1.

Figure 1 shows representative examples of environmental, genetic and GxE effects. Expression levels of Heme Oxygenase-1 (*Hmox1*) are shown in Figure 1A for cells in control and OxPAPC-treated cells in different mouse strains, and in Figure 1B for cells in control and LPS-treated cells. *Hmox1* expression is strongly regulated by environmental inflammatory stimuli in response to OxPAPC ($p < 1 \times 10^{-16}$), but not in response to LPS. In contrast, expression of N-acetylneuraminic pyruvate lyase (*Npl*) is strongly influenced by genetic effects (Figure 1C, $p < 1 \times 10^{-16}$), but not by environmental effects in response to LPS ($p = 0.37$). The expression levels of Interferon activated gene 205 (*Ifi205*) are influenced by environmental effects (Figure 1D, $p < 5.17 \times 10^{-6}$), genetic effects ($p < 1 \times 10^{-16}$) and show a GxE interaction ($p < 1 \times 10^{-16}$).

We used DAVID gene ontology to identify pathways and cellular processes enriched in genes regulated by inflammatory stimuli. Consistent with previous work, we found that phosphoproteins ($p = 2.5 \times 10^{-23}$), Toll-like receptor signaling ($p = 5.1 \times 10^{-9}$) and NOD-like receptor signaling ($p = 4.1 \times 10^{-6}$) were highly enriched in response to LPS, while regulation of kinase activity ($p = 4.7 \times 10^{-5}$), cytokine production ($p = 3.7 \times 10^{-5}$) and SH2 domain ($p = 1.8 \times 10^{-4}$), which recognizes phosphorylated tyrosine residues, were enriched in response to OxPAPC. Genes that were regulated by OxPAPC and not by LPS were enriched in glutathione metabolism ($p = 1.5 \times 10^{-5}$) and response to oxidative stress ($p = 9.5 \times 10^{-3}$), consistent with the hypothesis that oxidative stress plays a major role in chronic inflammatory disorders such as atherosclerosis. In contrast, genes regulated by LPS and not by OxPAPC were enriched in phosphoproteins ($p = 1.2 \times 10^{-20}$) and the Toll-like receptor pathway ($p = 1.4 \times 10^{-8}$).

The complete list of genes, fold-induction, Anova p -values and FDRs can be found in the online database, and similar plots as those shown in Figure 1 to examine the response to LPS or OxPAPC for all genes represented in the array.

Association mapping of gene expression

To identify genetic loci responsible for inflammatory responses and GxE interactions, we performed association mapping of genome-wide expression levels using single nucleotide polymorphisms (SNPs) across the mouse genome. For each gene we associated differences in gene expression to genetic differences using Efficient Mixed Model Association (EMMA). We and others have previously shown that EMMA effectively reduces false positive associations due to population structure among the mouse inbred strains (Bennett et al., 2010; Kang et al., 2008), thus allowing us to identify genomic loci that regulate the mRNA expression levels of any given gene represented in the microarray. These loci are commonly referred to as expression Quantitative Trait Loci, or eQTL.

We observed dramatic differences in the eQTL identified in control, LPS and OxPAPC-treated macrophages (Figure 2 and Table S2). We found both *local* or *cis*-eQTL, where expression levels of a gene were regulated by genetic variation at or near that same gene, as well as *distant* or *trans*-eQTL, where expression levels of a given gene were controlled by variation at a different locus, likely representing regulatory relationships between the genes. Most of the loci we identified in *trans* belonged to the LPS-treated macrophages (18,082), followed by 11,658 loci identified in control-treated cells, and 9,344 loci identified in OxPAPC-treated cells, at the 5% FDR level. We also found a large number *cis* associations, 5,217 in the control, 4,587 in LPS and 4,747 in the OxPAPC conditions.

Treatment-specific associations represent an interaction between genetics and the environment, where specific differences in gene expression are only observed in the context of an external stimulus. To specifically examine genetic loci influenced by GxE interactions, we mapped the fold difference between LPS-treated and control gene expression levels, or the fold difference between OxPAPC-treated and control expression levels. We found 4,805 *gxe*QTL in LPS and 81 *gxe*QTL in OxPAPC conditions in *trans*, as well as 1,394 *cis-gxe*QTL in response to LPS and 219 *cis-gxe*QTL in response to OxPAPC (Table S2 and Figure S3). For example, *Ifi205* is a gene that shows a *gxe*QTL in *cis* (Figure 1D), while *Abca1* shows a *gxe*QTL in *trans* (Figure 5A and 5B) in the LPS condition. Genes with *gxe*QTL in LPS but not in OxPAPC were highly enriched for acetylation ($p < 8.2 \times 10^{-25}$), phosphoprotein ($p < 3.2 \times 10^{-18}$) and mitochondrial proteins ($p < 4.4 \times 10^{-15}$) using gene ontology. We did not find significant gene ontology enrichments in the OxPAPC *gxe*QTL.

Type I and Type II errors in association studies can be due to the influence of confounders such as population structure and batch effects. These can result in an inflation (too many false positives) or deflation (too many false negatives) in the association results. We used EMMA to control for spurious associations due to population structure, and to verify that there was no inflation, we computed the inflation factor lambda. Lambda values over 1 indicate inflation, lambda values under 1 indicate deflation, and lambda of 1 indicates neither. We computed the inflation factor in our association results and observed no evidence of inflation, with lambda values ranging from 0.9–1 (Table S2). Association results for all genes and all conditions can be found on our online database.

Expression “hotspots”

Previous studies on the genetics of gene expression have suggested the existence of eQTL “hotspots”, where a polymorphism(s) at a locus is responsible for changes in gene expression in tens or hundreds of genes (Ghazalpour et al., 2008). These can be seen as vertical bands in the plots of genome-wide association of gene expression (Figure 2), where hundreds of transcripts across the genome were all associated with a SNP(s) in a locus. To find eQTL hotspots, we divided the genome into 2-Mb size bins and counted the number of *trans*-eQTL genes mapping to each bin.

We observed striking differences in hotspots from cells exposed to the different stimuli. We found 54 significant hotspots in control-treated cells, 47 hotspots in LPS, 39 hotspots in OxPAPC, 17 hotspots for LPS *gxe*QTL and no hotspots in OxPAPC *gxe*QTL (Figure 3 and Figure S4). The majority (145/157) of the hotspots regulated less than 1% of all eQTL in each condition, and only 3 hotspots, identified in response to LPS, regulated more than 5% of eQTL. A complete list of eQTL hotspot genome positions, their significance and the number of genes regulated by each hotspot can be found in Table S3 and in our online database. We identified several common hotspots in the different conditions. Although we found a significant overlap in the transcripts mapping to hotspots that overlap in different conditions, the majority of the transcripts mapping to each hotspot were specific to the treatment condition. The number of hotspots which overlap in the different conditions can be found in Table S4 and in our online database.

The finding of an eQTL hotspot suggests the presence of a regulator(s). We found a total of eight unique hotspots with profound changes in gene expression across the genome, affecting more than 1% of all eQTL. Three of these mapped to previously known regulators of inflammatory responses, including Tumor necrosis factor alpha, *Tnf*, in the hotspot at 34–36 Mb on chromosome 17 for LPS-treated cells and in the LPS-response *gxe*QTL. We also found a cluster of *Serpin* genes adjacent to a hotspot at 110–112 Mb on chromosome 1 in the LPS and LPS-response conditions. *Serpinb2*, which plays a role in adaptive immunity

(Schroder et al., 2010), is a candidate causal regulator for this locus. Finally, Interleukin 1a (*Il1a*) and Interleukin 1b (*Il1b*) in an OxPAPC-specific hotspot at 128–130Mb on chromosome 2. These observations suggest that the eQTL hotspots we identified are biologically meaningful, and hence that the hotspots in loci not previously implicated in inflammation will likely reveal novel regulators of inflammation.

Expression “hotspots” reveal a novel regulator of inflammatory responses

To identify novel regulators of inflammatory responses, we experimentally validated one of the hotspots in LPS-treated cells. The locus is in mouse chromosome 8 at approximately 119Mb and controls a large number of eQTL, 6% of eQTL in LPS and 13.5% of LPS *gxe*QTL. There are 12 candidate genes in the locus based on the LD structure. To narrow down the list of candidate genes for experimental validation, we selected genes that showed a difference in expression among the strains and genes with documented coding non-synonymous SNPs, and excluded genes whose expression was undetectable by quantitative PCR (qPCR) in primary macrophages. These criteria narrowed down our list to six genes: *2310061C15Rik*, *4933407C03Rik*, *Atmin*, *Gcsh*, *1700030J22Rik* and *Gan*. Among these, *2310061C15Rik* had a strong *cis*-eQTL in LPS-treated cells ($p=1.9\times 10^{-9}$).

For experimental validation, we used siRNA to knock-down expression levels in each of the six candidate genes in primary mouse macrophages treated with LPS. We were successful in obtaining approximately 50% knock-down in four of the candidates, *2310061C15Rik*, *4933407C03Rik*, *Atmin* and *Gcsh*. However, despite repeated attempts, we were unable to obtain consistent knock-down of either *1700030J22Rik* or *Gan*, possibly due to the low level of expression in the case of the *1700030J22Rik* gene. To assess the effect of knock-down on *trans*-eQTL genes predicted to be regulated by the chromosome 8 locus, we measured expression of 19 *trans*-eQTL genes by qPCR. In these initial experiments, we saw that 8 of the 19 genes tested (42%) were validated reproducibly, and their expression was affected by knock-down of either *2310061C15Rik* in 6 of the 8 genes, or *Gcsh* in 2 of the 8 genes. We did not observe reproducible differences in the 19 *trans*-eQTL genes after knock-down of the other candidate genes.

To more comprehensively validate the chromosome 8 hotspot, we examined global gene expression using microarrays. For this, we again used siRNA to knock-down the two candidate genes *2310061C15Rik* and *Gcsh*, since they showed the highest effect on target genes by qPCR. We profiled the transcriptome after knock-down using microarrays and determined how many of the genes that mapped to the chromosome 8 hotspot locus as eQTL were affected by the knock-down (Figure 4). Knock-down of *2310061C15Rik* or *Gcsh* had a significant effect on 173 and 128 genes, respectively (Figure 4A and Table S5). The number of genes affected in each knock-down experiment was significantly higher than expected by chance based on random samplings in LPS-treated cells ($p=1.11<1\times 10^{-16}$ for *2310061C15Rik* and $p<1\times 10^{-16}$ for *Gcsh*). Similar results were observed for the LPS-response condition (Table S5).

To assess the functional significance of genes validated in each knock-down experiment, we looked at the GO enrichment terms for each list. The GO enrichments for genes influenced by siRNA knock-down of *2310061C15Rik* were immune response ($p=9.3\times 10^{-11}$), regulation of T-cell activation ($p=7.0\times 10^{-5}$), cytokines ($p=2.0\times 10^{-4}$) and Toll-like receptor signaling ($p=4.0\times 10^{-4}$) in the LPS condition, and included inflammatory cytokines and LPS primary response genes such as *Il1b*, *Csf1*, *Il6*, *Ccl2* (MCP-1) and *Serpine1* (Figure 4B). In contrast, the genes influenced by siRNA knock-down of *Gcsh* were enriched in GTPase activity ($p=3.3\times 10^{-3}$) and were not enriched in immune response or Toll-like receptor signaling ($p=0.62$). Our validation results confirm that the chromosome 8 eQTL hotspot

represents biologically meaningful regulatory relationships between candidate genes and *trans*-eQTL mapping genes. However, we also observed that more than one gene in the locus was responsible for regulation of the *trans*-eQTL. Finally, our results indicate that *2310061C15Rik* is a novel regulator of inflammatory responses underlying the chromosome 8 eQTL hotspot.

Using eQTL to find regulatory relationships and candidate gene identification

One of the goals of systems genetics is to understand the behavior of the system as a whole by identifying all the elements present in the system and understanding the relationships among them. The eQTL identified in our study provide a suitable resource to understand the gene expression regulatory circuits present in macrophages when they are exposed to inflammatory stimuli such as LPS and OxPAPC. This information can also be used to understand the biological networks underlying traits with an inflammatory component. Towards this end, we have developed an online database, and below we describe how it facilitates discovery of new and/or pre-existing relationships among genes and clinical traits.

Gene expression, correlations, GxE and eQTL

Here are some of the types of data that can be obtained for any gene of interest represented in the array, as an example for *Abca1*: (1) a user can query and download our results for genetic, environmental and GxE effects in tabular or graphical format (Figure 5A). The tabular format includes Anova *p*-values, FDR, the average fold-change in response to a treatment and the number of strains which show a fold difference above two for each of the conditions. (2) The user can query the results for gene-gene expression correlations between the gene of interest and all other genes in tabular format. (3) A user can query all eQTL association results for the gene of interest, in any of the conditions, in tabular or graphical format (Figure 5B). The tabular format also conveys detailed information such as the *p*-value for the association, specific SNP name and coordinates, and links to the UCSC genome browser at that locus. (4) One can also obtain gene expression profiles, correlations and eQTL results from additional tissues (liver and bone) previously profiled in the HMDP, and compare expression in macrophage control, LPS, OxPAPC, to adipose, aorta, heart and liver for a gene of interest (Figure 5C). Similarly, one can obtain results for correlations, eQTL or clinical QTL from additional genetic studies in mouse intercrosses and in human endothelial cells exposed to OxPAPC. All of these can be used to compare and contrast results between these data sets and the macrophage data set presented here.

Regulatory relationships between genes

Our database allows us to screen for novel genes that regulate a gene of interest using *trans*-eQTL for the gene. Each *trans*-eQTL is hypothesized to harbor at least one gene (e.g. geneA) that is responsible for modulating the expression of a gene of interest (e.g. geneB). However, since the locus may carry more than one gene (e.g. several genes can be geneA), the limiting step in identifying such interactions is to select the appropriate candidate regulator. To do this, we can use various parameters such as: linkage disequilibrium, to define the physical boundaries of the locus; the median expression of the genes in HMDP strains to exclude genes which are very lowly expressed in the cell; presence of *cis*-eQTL, to select genes which vary in expression in HMDP strains as a result of genetic variation in or near the gene; coding non-synonymous SNPs, to select genes which have structural variation; and previously documented relationships in the published literature.

As an example, we used *trans*-eQTL and the various criteria described above to establish putative regulatory relationships for *Abca1*, a gene involved in reverse cholesterol transport

(Figure 6). Expression of *Abca1* maps to four different loci in LPS-treated cells (Figure 5B). A locus on chromosome 17 contains *Tnf*, a gene known to regulate *Abca1* (Edgel et al., 2010). The locus on chromosome 4 contains toll-like receptor 4, *Tlr4*. Although previous studies have suggested a connection between toll-like receptor signaling and cholesterol efflux pathways (Zhu et al., 2010), our observed *trans*-eQTL suggests that *Abca1* itself is regulated by *Tlr4*. Another locus on chromosome 17 is roughly 1 Mb away from *Lnpep*, a gene involved in cholesterol metabolism, which suggests regulation of *Abca1* by *Lnpep*. Based on a fourth *trans*-eQTL, *2310061C15Rik* is also hypothesized to regulate *Abca1*, since there is a *cis*-eQTL for the candidate gene *2310061C15Rik*. Similarly, extending the network connections to known published associations and novel associations found through the *trans*-eQTL in our data set, created a link between reverse cholesterol transport and adipogenesis via *Pparg* and *Adipor2* (Chinetti et al., 2004; Hamm et al., 1999). Also, combining known relationships with novel *trans*-eQTL extends the connections of *Abca1* to a host of inflammatory mediators through *Tnf* (Figure 6). In particular, two candidate genes underlying eQTL hotspots, on chromosome 1 (*Serpinb2*) and 8 (*2310061C15Rik*) demonstrated high degree of interaction with inflammatory mediators and with each other (Figures 6 and Figure S5), since *Serpinb2* maps to *2310061C15Rik* in the chromosome 8 hotspot.

Identification of positional candidate genes involved in inflammation

Our database of macrophage eQTL can also be used to prioritize genes involved in complex traits. Macrophages play critical roles in many conditions that involve acute and chronic inflammation, such as susceptibility to infection and atherosclerosis, and previous studies have identified hundreds of regions in the genome that are linked to immune-related traits in mice, i.e. clinical QTL. The QTL identified in these studies harbor a causal gene(s) influencing the trait of interest. Our online database allows one to narrow down candidate genes in clinical QTL, by looking for genes with a *cis*-eQTL in a region of interest. To illustrate this utility, we obtained genomic coordinates for previously identified QTL from Biomart and used *cis*-eQTL to prioritize candidate genes.

We found *cis*-eQTL candidate genes in 145 immune-related clinical traits, which have been previously identified in mouse QTL studies. In total, we identified 514 candidate genes for these 145 clinical QTL. These include atherosclerosis (Figure 7A), susceptibility to *Salmonella typhimurium* (Figure 7B), systemic lupus susceptibility, autoimmune susceptibility, arthritis, response to trypanosome infection, leishmaniasis resistance, cytokine production and TNF-lethal shock susceptibility. Candidate *cis*-eQTL mapping genes in atherosclerosis QTL are shown in Figure 7A. Interleukin 10 has been shown to play a role in atherosclerosis (Mallat et al., 1999), and we found a related gene, Interleukin 10 receptor a (*Il10ra*) as a candidate gene for the atherosclerosis QTL in mouse chromosome 9 at 44–46 Mb. We also found the gene *2310061C15Rik*, which we examined above in an eQTL hotspot, as a candidate *cis*-eQTL for the atherosclerosis QTL in mouse chromosome 8, identified in a cross between strains C57BL/6J and A/J. Based on our findings, this gene regulates the expression of several inflammatory genes and is likely to contribute to atherosclerosis.

We identified several candidate *cis*-eQTL mapping genes in QTL for susceptibility to *S. typhimurium* (Figure 7B). These include genes with previously described functions in immunity, such as *Ifi204* in the distal mouse chromosome 1 QTL, the NOD-like receptor family genes *Naip1*, *Naip2* and *Naip5* in the distal chromosome 13 QTL, and the lymphocyte antigen genes *Ly6a* and *Ly6d* in chromosome 15. We also found that *Ppp3ca* and *Dok1* are candidate genes, and although no role in susceptibility to infection has been described for these genes, *Ppp3ca* gene targeted mice show decreased T-cell proliferation (Zhang et al., 1996), and *Dok1* null mice show increased response to LPS (Shinohara et al.,

2005). A complete list of candidate genes for each of the 145 immune-related clinical QTL we examined can be found in our online database.

DISCUSSION

The finding of common genetic interactions has important implications for the study of common diseases and other complex traits. Human genome-wide association studies are poorly powered to identify genetic interactions and, thus, human geneticists have tended to ignore them. But studies in mice suggest that gene-gene and gene-environment interactions are prevalent, and our results are consistent with that conclusion. Heritability calculations in human studies assume an additive model and, if common disease traits have a large non-additive component, this would substantially inflate the heritability estimates (Zuk et al., 2012). Interactions add a level of complexity that may have broad implications for the development of treatments and for diagnosis. Nevertheless, the use of the HMDP to detect genetic effects is limited to identifying common genetic variants, as opposed to rare or strain-specific effects, similar to human GWAS. This limitation is inherent to the current panel of HMDP strains and to the use of genome-wide association itself. Additional studies in more strains, in humans, and using DNA sequencing will complement the current work and help us identify rare variants influencing inflammatory phenotypes.

Overall, our data strongly support that GxE interactions play a major role in the regulation of genome-wide gene expression and inflammatory responses. We observed that the expression of thousands of genes was regulated by naturally occurring genetic variation or environmental stimuli. A large proportion of these were also controlled by GxE interactions in LPS and OxPAPC (Table S1 and S2), with a much more robust response to LPS than to OxPAPC. It is possible that the reason we found the majority of the *gxe*QTL in the LPS condition is that LPS elicits more robust changes in gene expression in the cell, and hence we have more power to detect these. Macrophages may show a minimal response to OxPAPC, or they may respond only after prolonged exposure to OxPAPC. Additional time-dependent genetic studies are still required to further elucidate the macrophage response to OxPAPC.

We observed several eQTL hotspots which controlled a large fraction of all eQTL (>5%) only in the presence of LPS, but not in control or OxPAPC conditions. In these environmental specific eQTL hotspots, we found both known and novel regulators of inflammation. We used a treatment specific eQTL hotspot to identify *2310061C15Rik* as a novel regulator of inflammatory responses. This was supported by: (1) *trans*-eQTL which map to the hotspot were highly enriched in Toll-like receptor signaling, immune response genes and cytokines; (2) there was an LPS treatment-specific *cis*-eQTL for the expression of *2310061C15Rik*, suggesting that it was a strong candidate gene for the locus; (3) *trans*-eQTL mapping genes were differentially expressed when we silenced expression of candidate genes using siRNAs (Figure 4); (4) the genes affected by knock-down of *2310061C15Rik* were enriched in immune response genes.

Numerous studies have identified eQTL hotspots in genetically diverse populations (Ghazalpour et al., 2008), but very few eQTL hotspots have been experimentally validated in yeast (Zhu et al., 2008), while none have been validated in mammals. This lack of validation may be due to a variety of reasons, such as GxE interactions. Synergistic and compensatory effects can also account for lack of validation, since one may need to simultaneously target two or more genes to observe an effect in some of the *trans*-eQTL genes. Hotspots may be complex loci, and we also found *Gcsh* as yet another candidate gene at the chromosome 8 hotspot. Both *2310061C15Rik* and *Gcsh* combined could only account for the regulation of approximately 12% of the total genes that mapped to this locus. The

remaining 88% genes may be regulated by other candidate genes not validated in this report. Also, the siRNA knock-down experiments we performed may not exactly mimic the life-long effects of natural genetic variation on cellular processes. Likewise, the 50% knock-down in expression of candidate genes we achieved may not be sufficient to observe an effect on *trans*-eQTL genes, or some of the siRNAs may have off-target effects. Finally, lack of validation may be due to false positives.

Although very little is known about the biology of *2310061C15Rik*, domain prediction algorithms show that it has homology to the mitochondrial protein Cytochrome c oxidase biogenesis protein *Cmc1*. Consistent with this, the LPS *gxe*QTL which map to the chromosome 8 hotspot were highly enriched in mitochondrial proteins ($p=5.3\times 10^{-6}$), and mitochondrial proteins and processes were the third most highly enriched category among all LPS eQTL ($p=6.3\times 10^{-15}$). Recent reports suggest that mitochondria integrate signals from infection and tissue damage, as well as signals from metabolic processes and reactive oxygen species to trigger an appropriate inflammatory response (Zhou et al., 2011). Notably, a previous linkage study for atherosclerosis found a locus which coincides with the physical location of *2310061C15Rik* on chromosome 8 (Chen et al., 2007). This warrants further work to investigate if genetically modified mice for the *2310061C15Rik* gene will exhibit differential susceptibility to atherosclerosis.

eQTL hotspots may be due to genetic differences that affect gene expression, protein structure, or regulatory elements that control expression of a causal gene(s). The causal genes may be transcription factors, or genes that affect transcription factor activity, such as the hotspot we found in chromosome 2, which maps to the cytokine Interleukin 1. We also observed that genes controlled by the chromosome 8 hotspot included transcription factors (e.g. *Irf1*), cytokines (e.g. *Il6*) and other regulatory proteins (e.g. *Mapk3*). Hence, we can speculate that a causal gene may influence expression of a target gene, which in turn regulates downstream genes in multiple regulatory pathways, so that a hotspot may reflect a signaling cascade triggered by the causal gene underlying the hotspot. It is also possible that eQTL hotspots are driven by epigenetic differences. Using reduced representation bisulfite sequencing in liver genomic DNA, we found over 2,000 CpG sites which vary in DNA methylation among mouse inbred strains (data not shown). The changes in DNA methylation levels were accompanied by differences in expression of nearby genes, and by nearby eQTL in 106 genes. These observations suggest that eQTL and eQTL hotspots are driven by genetic, environmental and also epigenetic differences among individuals.

We believe that our approach has some important advantages and builds upon concepts proposed in previous work. Studies in a mammalian model organism such as the mouse are directly applicable to biological processes and pathways in humans. Because the HMDP consists of permanent inbred strains, we propose that the data generated here constitute a cumulative resource that can be used for the integration of genetic, gene expression and phenotype data for the understanding of complex immune-related traits. In conclusion, we observed that gene-by-environment interactions occur abundantly throughout the genome. As such, the combined success and failure of any GWAS study, as we have witnessed in recent years, will be largely linked to the functional dependency of causal variants to the environmental conditions, and how these variants interact with them.

EXPERIMENTAL PROCEDURES

Online database

Results can be accessed at <http://systems.genetics.ucla.edu/data>

Accession numbers

All microarray data from this study are deposited in the NCBI GEO (<http://www.ncbi.nlm.nih.gov/geo/>) under the accession number GSE38705.

Mice

Male mice were obtained from the Jackson Laboratories (Bar Harbor, ME). Mice were housed in pathogen-free conditions according to NIH guidelines until 16-weeks of age, then fasted overnight for 16 hours prior to euthanasia. A complete list of strains can be found in Table S6 and in the online database.

Macrophage culture conditions

We harvested primary macrophages using four mice per strain, by intraperitoneal lavage four days after injection with thioglycollate (BD, Sparks, MD). All mice were injected with the same batch of thioglycollate. We pooled cells from different mice of the same strain, and plated duplicates or triplicates per condition, per strain. We used additional replicates for some of the strains to determine experimental reproducibility (Table S6). The next day, cells were incubated for 4 hours with 1% FBS DMEM media in control-treated cells, media plus 2ng/mL LPS (List Biological Inc., Campbell, CA), or media plus 50µg/mL OxPAPC.

Expression array profiling

We profiled RNA using Affymetrix HT MG-430A arrays, from 86 strains in control, 89 in LPS and 80 in OxPAPC-treated cells (Table S6). We used the Robust Multichip Average (RMA) method to determine the hybridization signals.

Reproducibility of microarray data

We arrayed different samples of the same strain in two different experiments for five strains in the LPS condition, and for seven strains in the control condition. We used hierarchical clustering of samples using all microarray data and the 'spearman' distance metric. To examine the distribution of the variance in gene expression, we computed the variance for each gene, using all strains treated with LPS for inter-strain variance, and all samples for a given strain for the intra-strain variance. We plotted the empirical cumulative distribution of these variances and compared the distributions using the Kolmogorov-Smirnov test. We took the mean of each variance distribution to compare the fold difference of the distributions.

Viability assay

We obtained macrophages from 4 strains in this study and 5 strains from the HMDP not included in this study (see Supplementary Experimental Procedures and Figure S2). We treated the cells the next day using control or LPS media for 4 hours and then incubated them with the cell permeable dye 2µM calcein AM (Molecular Probes). As a negative control, we added 70% methanol to control-treated cells to kill the cells, and then incubated them in calcein AM. We read the fluorescent intensity at 530nm. We compared the two groups using a *t*-test.

Environmental and genetic analysis of variance

To examine genetic effects, we used one-way Anova for each of the transcripts in the array in strains treated with control, and used the strain label as the grouping label variable, as previously described (Smith and Kruglyak, 2008). For environmental effects, we compared control versus treated samples using one-way Anova and the treatment label as the variable. To find genes that were regulated by at least one treatment, we compared all samples using

one-way Anova with three grouping variables (control, LPS and OxPAPC). For GxE interactions, we used a two-way Anova with interaction model, using strains in all treatments, with both treatment and strain labels as the variables. We calculated FDR for each of the effects and selected genes with $FDR < 5\%$. For GxE interactions, we selected genes significant for GxE effects, genetic and environmental effects. Since there are genes with more than one microarray probe-set, we reported the number of unique genes, that were regulated at least 2-fold in at least 5 strains.

Genetic association and genotyping

Genotyping—Mouse inbred strains were previously genotyped by the Broad Institute (www.broadinstitute.org/mouse/hapmap) and the Wellcome Trust Center for Human Genetics. We selected informative SNPs with a minor allele frequency greater than 10% and missing values in less than 10% of the strains for each SNP. This criteria resulted in 96,518 SNPs in control, 95,733 in LPS, 94,510 in OxPAPC, 95,649 in LPS-response and 94,210 in the OxPAPC-response conditions.

Association mapping—We used EMMA to test for association and to account for population structure and genetic relatedness among strains. We applied the linear mixed model: $y = \mu + x\beta + u + e$. Where μ =mean, x =SNP, β =SNP effect, and u =random effects due to genetic relatedness with $\text{Var}(u) = \sigma_g^2 K$ and $\text{Var}(e) = \sigma_e^2$, where K =IBS (identity-by-state) matrix across all genotypes in the panel. We computed a restricted maximum likelihood estimate for σ_g^2 and σ_e^2 , and we performed association based on the estimated variance component with an F-test to test $\beta = 0$.

Local and Distant eQTL definition—eQTL were defined as *Local* or *cis* if the peak association was within a 4Mb interval, flanking 2Mb on either side of the genomic start site of the gene. eQTL were defined as *Distant* or *trans* by selecting the peak association per chromosome per gene, excluding loci that mapped in *cis*.

Genome-wide alpha for cis-eQTL—We calculate false discovery rates using the *qvalue* package in R. For each gene, we selected all association *p*-values in the 4 Mb interval, and calculated *q*-values using all the *p*-values for all genes. We estimated the FDR separately for each treatment and selected $FDR < 5\%$ as follows: control $p < 8.88 \times 10^{-3}$, LPS $p < 6.74 \times 10^{-3}$, OxPAPC $p < 8.56 \times 10^{-3}$, LPS GxE $p < 1.15 \times 10^{-3}$ and OxPAPC GxE $p < 1.38 \times 10^{-4}$.

Genome-wide alpha for trans-eQTL—Due to the computational complexity associated with evaluating *q*-values for over 2 billion *p*-values, we computed the FDRs by taking the median FDR for 100 samples, each containing 5 million randomly selected *p*-values from the original calculated association *p*-values (Ghazalpour et al., 2008). We estimated the FDR separately for each treatment and selected $FDR < 5\%$ as follows: control $p < 1.09 \times 10^{-5}$, LPS $p < 9.58 \times 10^{-6}$, OxPAPC $p < 9.91 \times 10^{-6}$, LPS GxE $p < 1.10 \times 10^{-6}$ and OxPAPC GxE $p < 6.31 \times 10^{-8}$. Additional *p*-value thresholds for different FDR cutoffs can be found in Table S7 and online database.

Inflation—We calculated the inflation factor lambda by taking the chi-squared inverse cumulative distribution function for the median of the association *p*-values, with one degree of freedom (DF), and divided this by the chi-squared probability distribution function of 0.5 (the median expected *p*-value by chance) with one DF. Since it was not feasible to calculate this statistic using all *p*-values, for each data set we calculated lambda using a random sample of 1000 *p*-values, 1000 times, and took the average and standard deviation of lambda. We also selected 5 million *p*-values, 100 times in the LPS GxE condition and

obtained comparable results of in the 5 million p -value sets ($\lambda=0.987\pm 0.001$) and 1000 p -value sets ($\lambda=0.991\pm 0.074$).

eQTL hotspots

For each condition, we divided the genome into 2Mb windows (the average size of linkage disequilibrium blocks in the HDMP strains) and counted the number of genes with significant eQTL in each window. Consecutive windows were merged if tag SNPs in the windows were correlated with $r^2>0.5$. We used the Poisson distribution to determine if individual windows contained a larger than expected number of eQTL. Hotspots were considered significant if the number of genes with eQTL in a window was above 30 for control, 39 for LPS, 26 for OxPAPC, 21 for LPS *gxe* interaction and 5 for OxPAPC *gxe* interaction.

Knock-down experiments

We obtained macrophages from C57BL/6J mice as described above. The day after plating we added siRNAs (Qiagen) complexed with Lipofectamine LTX (Invitrogen, Carlsbad CA) to the cells for 6 hours, and then washed the cells. After 48 hours, we treated cells with control media or media plus LPS for 4 hours, then harvested total RNA. We determined the level of knock-down from cDNA using quantitative PCR (Roche, San Francisco CA), and normalized data using Rpl4 as an internal control. We used at least 2 siRNAs per candidate gene.

Analysis of knock-down data—For each candidate gene, we used one-way Anova to compare the scramble siRNA, and siRNAs to target the candidate gene, using the siRNA label as the grouping variable. We selected genes significant in the Anova test at the $FDR<5\%$ and that were affected by at least 2 of the siRNAs used for the same candidate gene, in the same direction, relative to the scrambled siRNA.

Random samplings—We carried out random samplings of transcripts in the microarray data. For each candidate gene knocked-down and random sampling, we selected significant genes in the same way we did for the non-random data above. We then repeated this analysis for 1,000 random samplings and determined the average number genes differentially expressed by chance (λ). To determine if our results were higher than expected by chance, we used the cumulative Poisson distribution, taking the number of genes differentially expressed in the non-random data (X) and λ .

Clinical QTL

We downloaded QTL information from Biomart (<http://biomart.informatics.jax.org/>) for immune related traits, and from Chen et al. for atherosclerosis QTL (Chen et al., 2007). We used the peak linkage position of the QTL and selected a 2Mb window around the QTL to search for *cis*-eQTL candidate genes, and selected all *cis*-eQTL physically located in the 2Mb window.

Supplementary Material

Refer to Web version on PubMed Central for supplementary material.

Acknowledgments

AJL and this work were supported by the NIH grants HL30568, HL28481 and D094311.

BB was supported by the NIH grant K99 HL102223.

CRF was supported by the Ruth L. Kirschstein NIH F32 Fellowship 5F32DK074317.

LDO was supported by USPHS National Research Service Award GM07104 and USPHS National Research Service Award T32-HG002536.

REFERENCES

- Bennett BJ, Farber CR, Orozco L, Kang HM, Ghazalpour A, Siemers N, Neubauer M, Neuhaus I, Yordanova R, Guan B, et al. A high-resolution association mapping panel for the dissection of complex traits in mice. *Genome Res.* 2010; 20:281–290. [PubMed: 20054062]
- Berliner JA, Leitinger N, Tsimikas S. The role of oxidized phospholipids in atherosclerosis. *J Lipid Res.* 2009; 50(Suppl):S207–S212. [PubMed: 19059906]
- Chen Y, Rollins J, Paigen B, Wang X. Genetic and genomic insights into the molecular basis of atherosclerosis. *Cell Metab.* 2007; 6:164–179. [PubMed: 17767904]
- Chinetti G, Zawadzki C, Fruchart JC, Staels B. Expression of adiponectin receptors in human macrophages and regulation by agonists of the nuclear receptors PPARalpha, PPARgamma, LXR. *Biochem Biophys Res Commun.* 2004; 314:151–158. [PubMed: 14715259]
- Edgel KA, Leboeuf RC, Oram JF. Tumor necrosis factor-alpha and lymphotoxin-alpha increase macrophage ABCA1 by gene expression and protein stabilization via different receptors. *Atherosclerosis.* 2010; 209:387–392. [PubMed: 19913791]
- Ghazalpour A, Doss S, Kang H, Farber C, Wen PZ, Brozell A, Castellanos R, Eskin E, Smith DJ, Drake TA, et al. High-resolution mapping of gene expression using association in an outbred mouse stock. *PLoS Genet.* 2008; 4:e1000149. [PubMed: 18688273]
- Hamm JK, el Jack AK, Pilch PF, Farmer SR. Role of PPAR gamma in regulating adipocyte differentiation and insulin-responsive glucose uptake. *Ann N Y Acad Sci.* 1999; 892:134–145. [PubMed: 10842659]
- Kang HM, Zaitlen NA, Wade CM, Kirby A, Heckerman D, Daly MJ, Eskin E. Efficient control of population structure in model organism association mapping. *Genetics.* 2008; 178:1709–1723. [PubMed: 18385116]
- Kanter JL, Narayana S, Ho PP, Catz I, Warren KG, Sobel RA, Steinman L, Robinson WH. Lipid microarrays identify key mediators of autoimmune brain inflammation. *Nat Med.* 2006; 12:138–143. [PubMed: 16341241]
- Mallat Z, Besnard S, Duriez M, Deleuze V, Emmanuel F, Bureau MF, Soubrier F, Esposito B, Duez H, Fievet C, et al. Protective role of interleukin-10 in atherosclerosis. *Circ Res.* 1999; 85:e17–e24. [PubMed: 10521249]
- Rojo L, Sjöberg MK, Hernandez P, Zambrano C, Maccioni RB. Roles of cholesterol and lipids in the etiopathogenesis of Alzheimer's disease. *J Biomed Biotechnol.* 2006; 2006:73976. [PubMed: 17047312]
- Romanoski CE, Lee S, Kim MJ, Ingram-Drake L, Plaisier CL, Yordanova R, Tilford C, Guan B, He A, Gargalovic PS, et al. Systems genetics analysis of gene-by-environment interactions in human cells. *Am J Hum Genet.* 2010; 86:399–410. [PubMed: 20170901]
- Schroder WA, Le TTT, Major L, Street S, Gardner J, Lambley E, Markey K, MacDonald KP, Fish RJ, Thomas R, et al. A Physiological Function of Inflammation-Associated SerpinB2 Is Regulation of Adaptive Immunity. *The Journal of Immunology.* 2010; 184:2663–2670. [PubMed: 20130210]
- Shinohara H, Inoue A, Toyama-Sorimachi N, Nagai Y, Yasuda T, Suzuki H, Horai R, Iwakura Y, Yamamoto T, Karasuyama H, et al. Dok-1 and Dok-2 are negative regulators of lipopolysaccharide-induced signaling. *J Exp Med.* 2005; 201:333–339. [PubMed: 15699069]
- Smith EN, Kruglyak L. Gene-environment interaction in yeast gene expression. *PLoS Bio.* 2008; 6:e83. [PubMed: 18416601]
- Wurfel MM, Park WY, Radella F, Ruzinski J, Sandstrom A, Strout J, Bumgarner RE, Martin TR. Identification of high and low responders to lipopolysaccharide in normal subjects: an unbiased approach to identify modulators of innate immunity. *J Immunol.* 2005; 175:2570–2578. [PubMed: 16081831]

- Zhang BW, Zimmer G, Chen J, Ladd D, Li E, Alt FW, Wiederrecht G, Cryan J, O'Neill EA, Seidman CE, et al. T cell responses in calcineurin A alphadeficient mice. *J Exp Med*. 1996; 183:413–420. [PubMed: 8627154]
- Zhou R, Yazdi AS, Menu P, Tschopp J. A role for mitochondria in NLRP3 inflammasome activation. *Nature*. 2011; 469:221–225. [PubMed: 21124315]
- Zhu J, Zhang B, Smith EN, Drees B, Brem RB, Kruglyak L, Bumgarner RE, Schadt EE. Integrating large-scale functional genomic data to dissect the complexity of yeast regulatory networks. *Nat Genet*. 2008; 40:854–861. [PubMed: 18552845]
- Zhu X, Owen JS, Wilson MD, Li H, Griffiths GL, Thomas MJ, Hiltbold EM, Fessler MB, Parks JS. Macrophage ABCA1 reduces MyD88-dependent Toll-like receptor trafficking to lipid rafts by reduction of lipid raft cholesterol. *J Lipid Res*. 2010; 51:3196–3206. [PubMed: 20650929]
- Zuk O, Hechter E, Sunyaev SR, Lander ES. The mystery of missing heritability: Genetic interactions create phantom heritability. *Proc Natl Acad Sci U S A*. 2012; 109:1193–1198. [PubMed: 22223662]

HIGHLIGHTS

A genetics study and database resource for dissecting molecular and clinical traits

Gene-environment interactions play a major role on the regulation of gene expression

Genome-wide responses to LPS and oxidized lipids in mouse macrophages

Validation of eQTL hotspot and identification of a novel regulator of inflammation

\$watermark-text

\$watermark-text

\$watermark-text

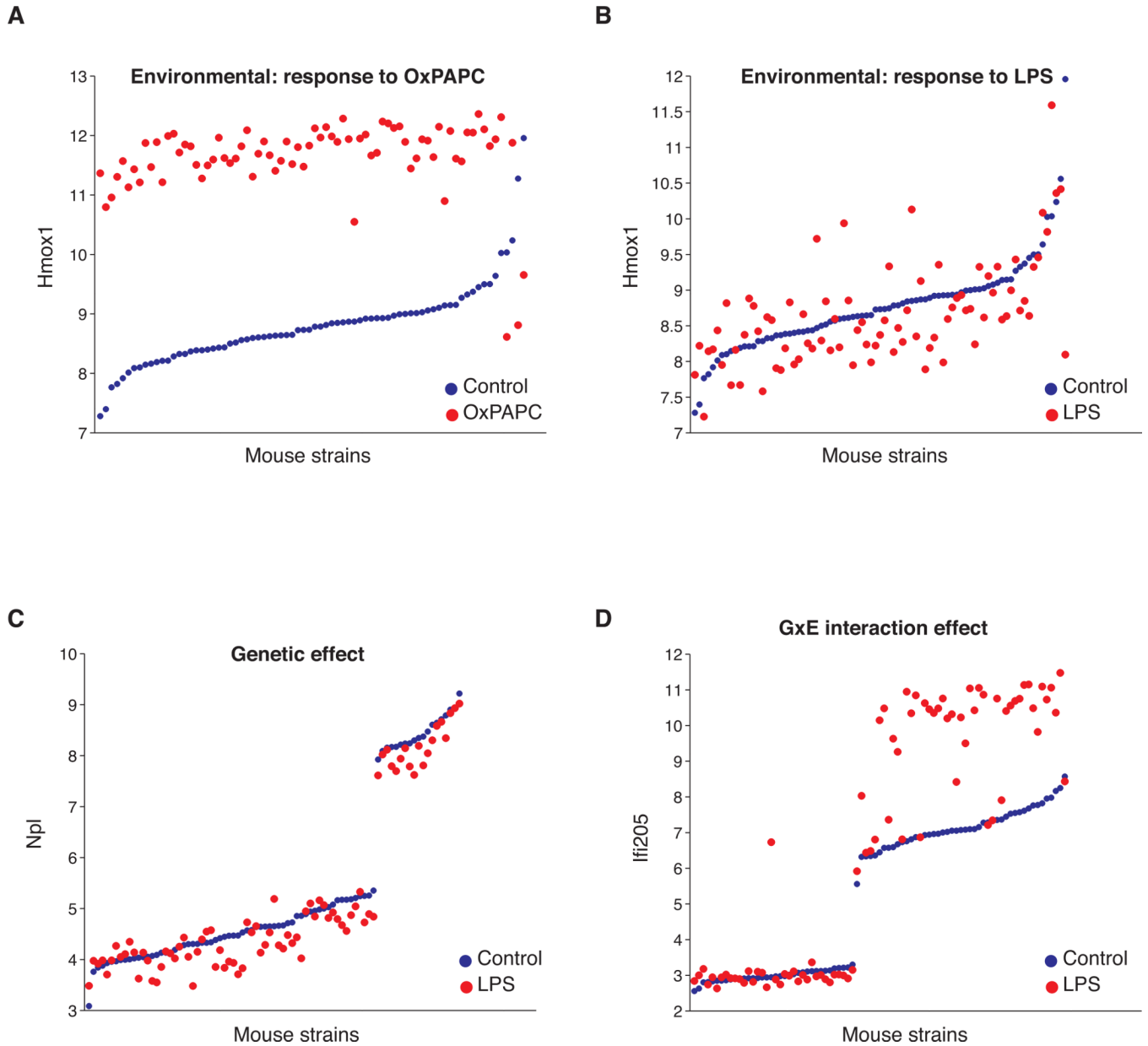


Figure 1. Environmental, Genetic and GxE interaction effects on gene expression

Expression levels are plotted as the log²(microarray intensity) on the Y-axis, for mouse strains on the X-axis. Each dot represents the levels of a gene for a given strain in control (blue dots) and treated cells (red dots). (A) *Hmox1* expression in response to OxPAPC and (B) *Hmox1* in response LPS, illustrate environmental effects. (C) *Npl* levels are influenced by genetic effects. (D) Expression levels of *Ifi205* are influenced by GxE interactions. See also Figures S1 and S2.

\$watermark-text

\$watermark-text

\$watermark-text

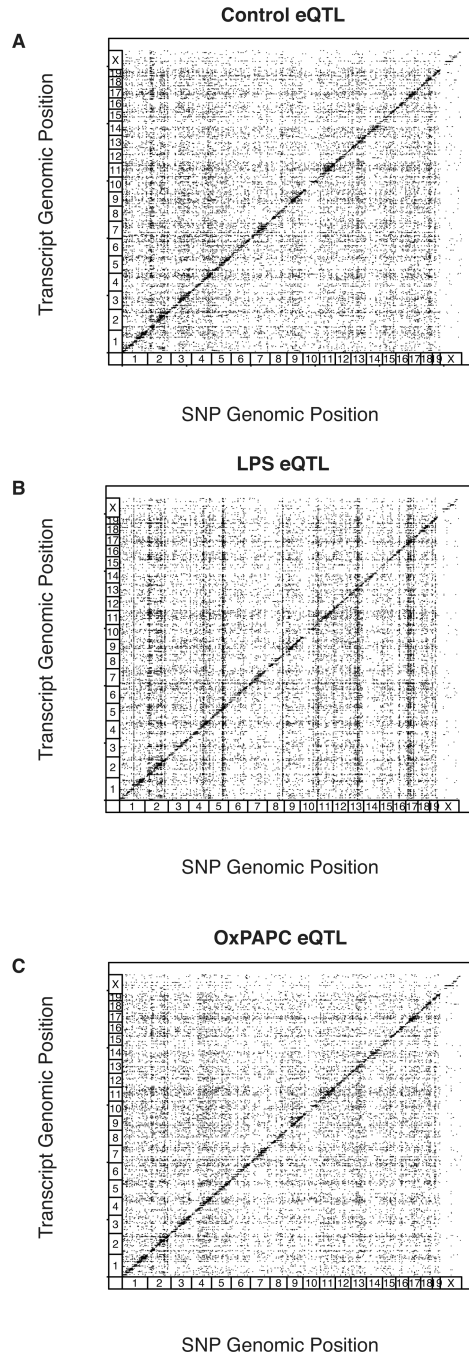


Figure 2. Genome-wide association of gene expression

Association using microarray expression of macrophages in various conditions. Each dot represents a significant association between a transcript and a SNP. Genomic position of the SNPs and transcripts are shown on the X and Y-axes, respectively. (A) Association in control condition. (B) Association in LPS condition. (C) Association in OxPAPC condition. See also Figure S3, Table S2 and Table S7.

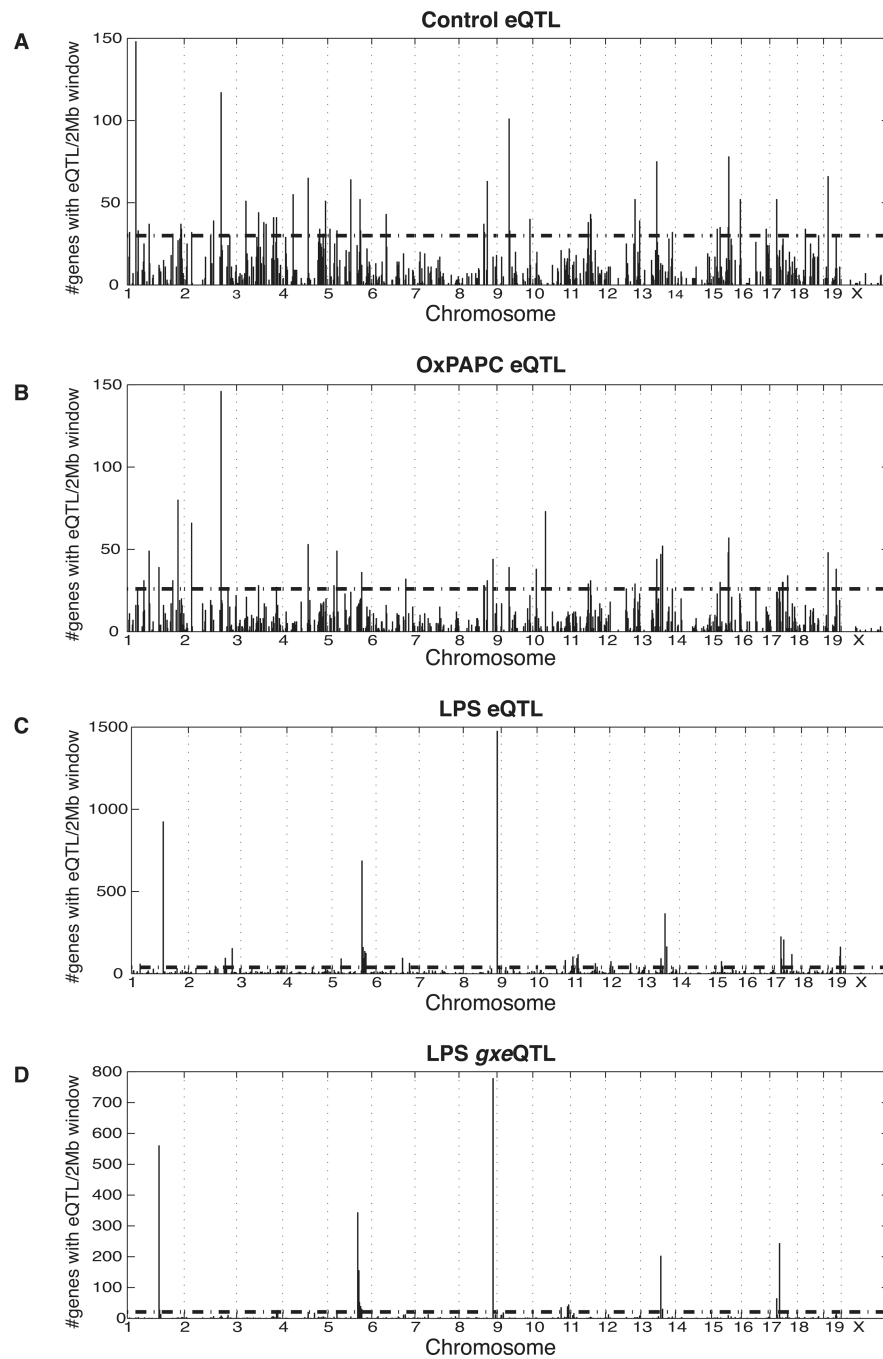


Figure 3. eQTL hotspots

The number of genes mapping to each 2-Mb bin is shown on the Y-axis and the genomic position of the bin is on the X-axis. The horizontal dashed line represents the significance threshold. (A) Hotspots in control eQTL. (B) Hotspots in OxPAPC eQTL. (C) Hotspots in LPS eQTL. (D) Hotspots in LPS *gxe*QTL. See also Figure S4, Table S3 and Table S4.

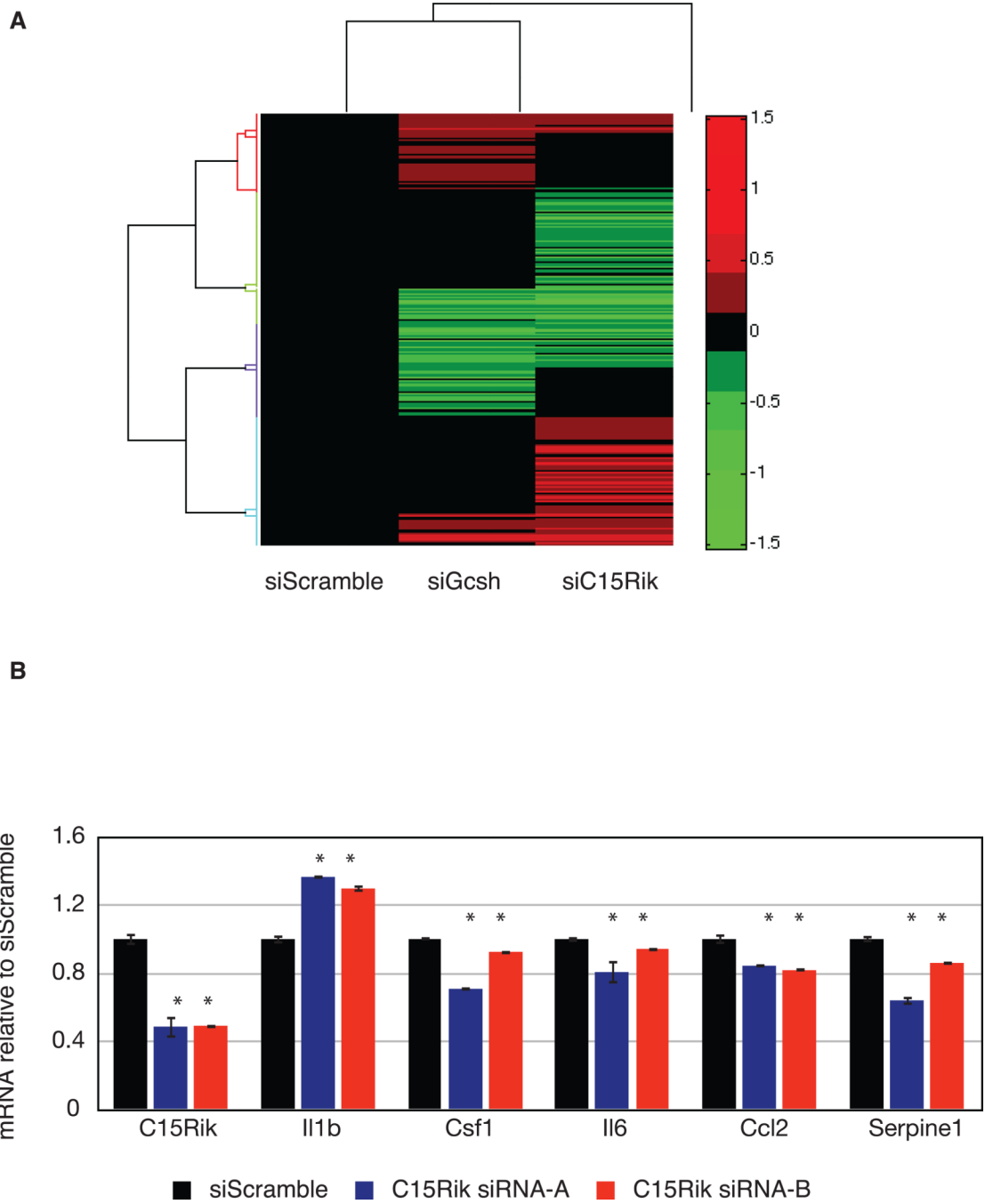


Figure 4. Expression levels in LPS condition after knock-down of candidate genes
 (A) Microarray expression levels in LPS condition for 273 genes affected by knock-down of the candidate genes *Gcsh* (siGcsh) and *2310061C15Rik* (siC15Rik). For each gene on the Y-axis, expression is plotted as the mean of the siRNAs (X-axis) that significantly affected expression relative to the scramble control on a log² scale. (B) Microarray expression levels for the genes *Il1b*, *Csf1*, *Il6*, *Ccl2* and *Serpine1*, after knock-down of the candidate gene *2310061C15Rik* (C15Rik). Data are presented as mean +/- standard deviation. See also Table S5.

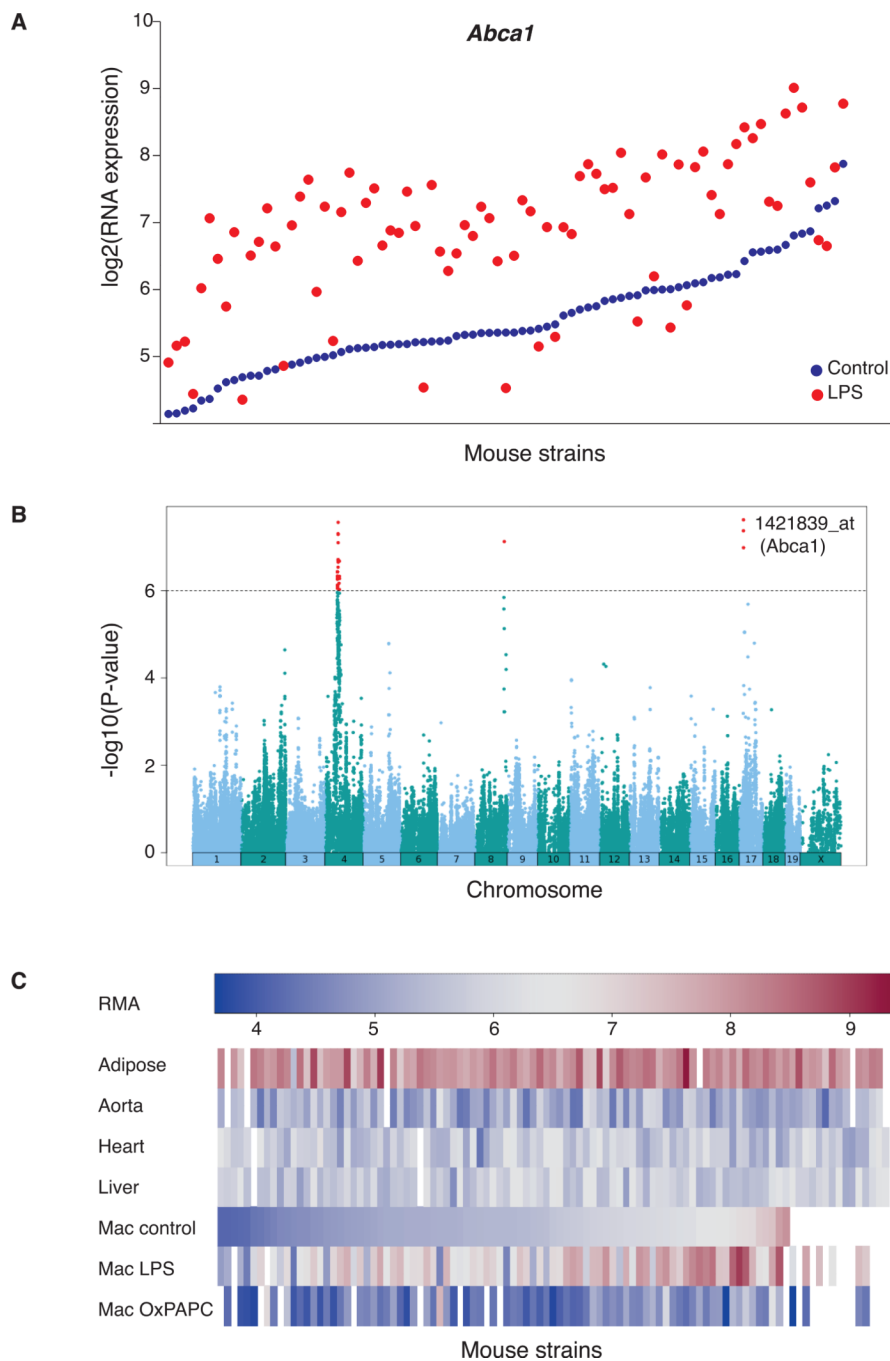


Figure 5. Database plots for *Abca1*

Sample plots for a given gene of interest that can be obtained from our online database. (A) LPS response of *Abca1*. (B) Genome-wide association for the expression of *Abca1*. (C) Relative expression levels among mouse strains of the HMDP in macrophages and different tissues.

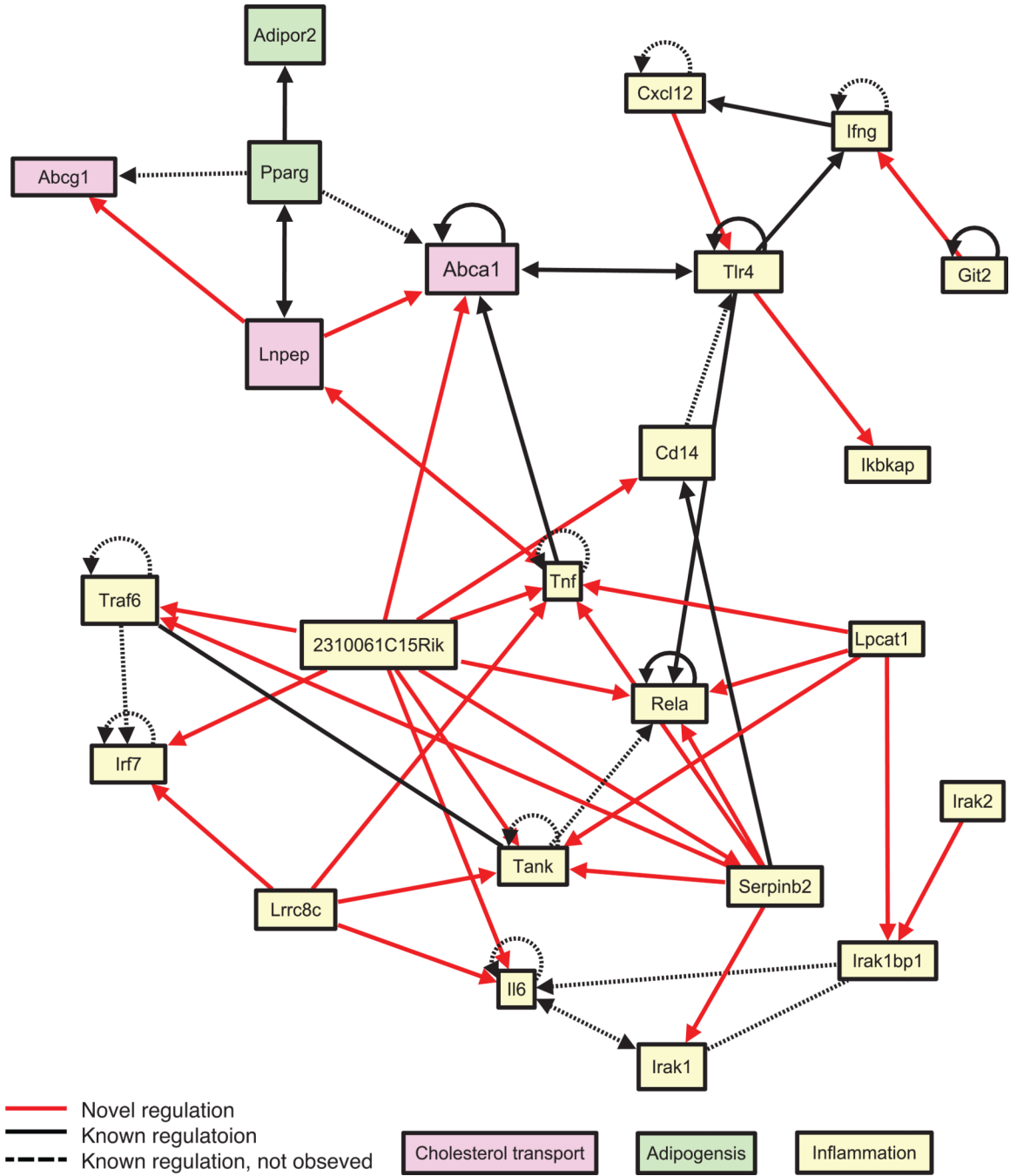


Figure 6. Abca1 and LPS-activation regulatory network defined by *trans*-eQTL
 Causal regulatory relationships between genes were defined using LPS *trans*-eQTL. Novel relationships are shown in red lines, and previously described relationships are in black lines. Dotted lines are previously described relationships which were not identified in the LPS *trans*-eQTL. See also Figure S5.

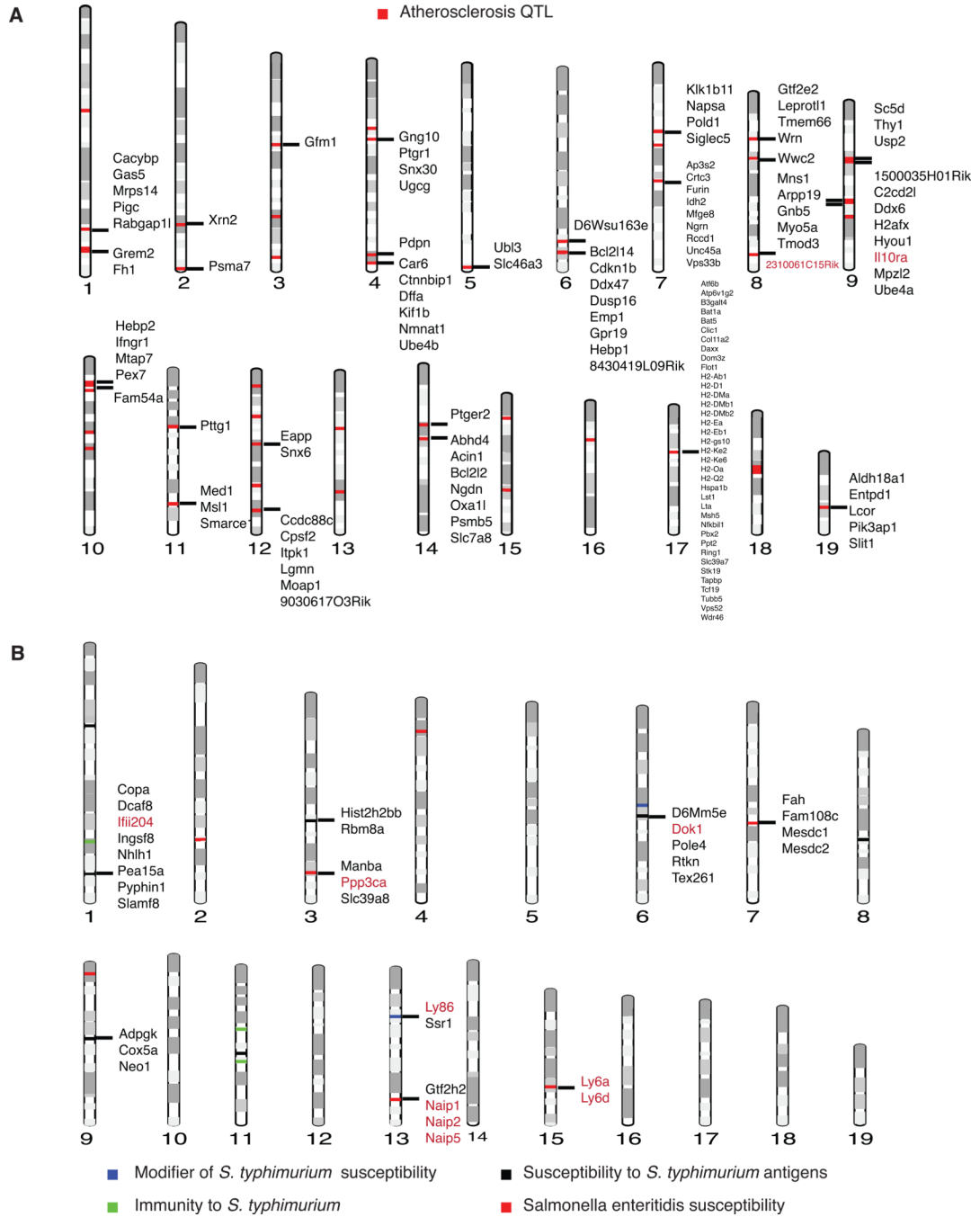


Figure 7. Candidate genes in QTL for Atherosclerosis and susceptibility to Salmonella typhimurium
 Ideograms of mouse autosomes showing the position of clinical QTL identified through multiple studies. The peak linkage region is marked with a red, blue, green or black bar. Genes listed for each QTL are *cis*-eQTL identified in this study. Genes discussed in the text are highlighted in red. (A) Atherosclerosis QTL. (B) QTL for susceptibility to *Salmonella typhimurium*.